

Article

Time-Dependent Probabilistic Approach of Failure Mode and Effect Analysis

Hyeon-ae Jang ¹ and Seungsik Min ^{2,*} ¹ Research & Business Foundation, Dong-A University, Busan 49315, Korea² Department of Natural Science, Korea Naval Academy, Changwon 51704, Korea

* Correspondence: fieldsmin@gmail.com; Tel.: +82-55-9075238

Received: 17 September 2019; Accepted: 13 November 2019; Published: 17 November 2019



Abstract: Failure mode and effect analysis (FMEA) is one of the most widely employed pre-evaluation techniques to avoid risks that may occur during product design and manufacturing phases. However, use of the risk priority number (RPN) in traditional FMEA results in difficulties being encountered with regard to quantification of the degree of risk involved. This study proposes the use of a probabilistic time-dependent FMEA (TD-FMEA) approach to overcome limitations encountered during implementation of traditional FMEA approaches. To this end, the proposed method defines the risk priority metric (RPM) as a priority decision value. RPM corresponds to the product of the expected loss and occurrence rate of the failure-cause. By assuming exponential and case functions for each occurrence and detection time instant, the expected loss corresponding to each failure-cause can be evaluated. Utility of the proposed approach has been described in the light of results obtained via its implementation during an automotive-manufacturing case study performed for the purpose of illustration.

Keywords: FMEA; TD-FMEA; RPN; RPM; expected loss; risk-evaluation

1. Introduction

Failure mode and effect analysis (FMEA) is an analysis technique for defining, identifying, and eliminating known and/or potential failures, problems, errors, etc. from systems, designs, processes, and/or services before they reach the customer [1]. The results of the FMEA can help analysts to identify and correct the failure modes that have a detrimental effect on the system and improve its performance during the stages of design and production [2]. Since its introduction as an analysis tool for reducing failures, FMEA has been extensively used in a wide range of industries, including automotive, semiconductor, aircraft medical, and steel industries [3–6].

In traditional FMEA approaches, the risk associated with a failure-cause is usually evaluated using the risk priority number (RPN), which corresponds to the mathematical product of the occurrence (O), severity (S), and detection (D) of a failure-cause (i.e., $RPN = O \times S \times D$, where O is related to failure occurrence, D to failure detection, and S to failure severity). RPN evaluation of a potential failure-cause requires evaluation of three risk factors via the use of the 1-to-10 scale. The higher the RPN of a failure-cause, the greater is the associated risk with regard to system/product reliability. However, this traditional FMEA risk-evaluation approach has often been extensively criticized in extant literature for a variety of reasons [2]. Noteworthy drawbacks of the traditional RPN-based approach include (i) no consideration of relative importance among O, S, and D parameters [7–10]; (ii) difficulties involved in precise evaluation of the three risk factors [5,11–17]; (iii) no consideration of interdependencies among different failure-causes and the corresponding effects [6,18–20]; and (iv) over-dependence on expert intuition and experience instead of scientific methods for evaluation of the three risk components [21,22].

Many researchers have attempted to overcome the above-mentioned drawbacks, thereby improving the FMEA risk-evaluation method in the process. Liu et al. [2] reported that the most popular FMEA approach corresponds to the fuzzy rule-based system [10,23–25], followed by the grey theory [9,10], cost-based model [11–13], AHP/ANP [7,19,26,27], and linear programming. Others included an integration-based approach [8,15–17,21,22,28] and probability-based methodology [14,29]. Apart from these approaches, the use of a time-dependent probabilistic approach for FMEA risk-evaluation has been proposed in this study. In the proposed model, two additional factors—time (failure occurrence and detection) and loss (repair and opportunity cost)—have been considered owing to them being directly associated with the criticality of the risks.

Typically, failures occur on account of the occurrence of even one of their causes. Additionally, occurrence of a failure may not be detected in real time, and there may exist some intermediate time delay. The loss incurred owing to the effect of a failure depends on this time delay. If a potential failure-cause can be detected prior to occurrence of actual failure, only a certain repair cost would be incurred. However, in the event of an actual failure, substantial monetary loss, including the expense due to failure and the corresponding repair cost, may be incurred. Figure 1 depicts typical scenarios of failure occurrence along with crude estimates of the expected loss depending on the time elapsed between failure occurrences and detection of their possible causes. The scenarios are based on the assumption that (i) each cause can independently lead to failure; (ii) the time elapsed between occurrence of a probable cause and that of the consequent failure is different in each case; (iii) the time required for detection of the failure-cause is different in each case; and (iv) failure effects are realized after failure occurrence. The failure-cause in case A is detected prior to failure occurrence. In case B, the failure-cause is detected long after failure occurrence, and this results in realization of significant failure effects. In general, it is well known that losses incurred after failure occurrence are much greater when compared to those incurred prior to failure occurrence. Thus, the risk involved in case B can be considered the greatest under the assumption that the failure effect per unit time remains the same in case A.

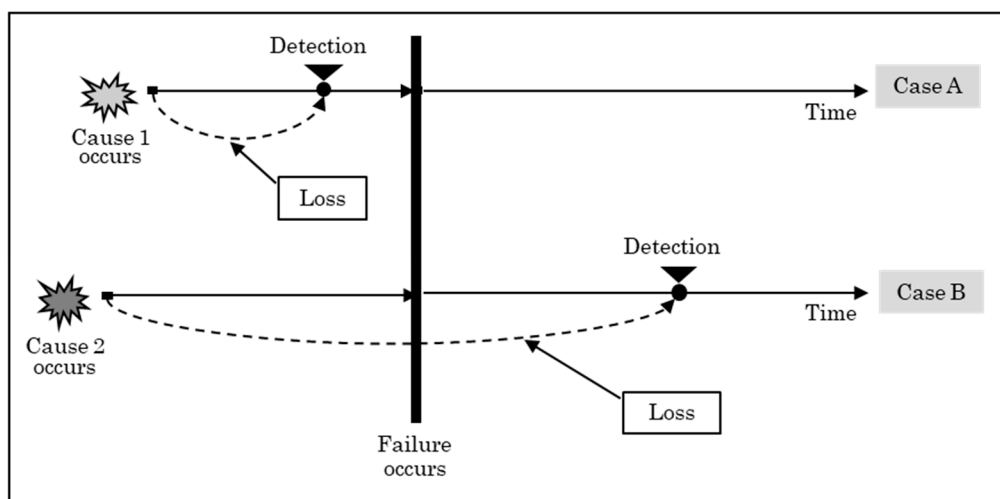


Figure 1. Effect of failure-cause detection time on the loss of a failure: If a detection is later than a failure, the loss increases rapidly.

In this study, a time-dependent probabilistic approach is proposed considering the real situation that the loss increases as detection of a failure or its causes late, and the risk of the failure-cause is quantitatively evaluated based on this. Assuming a case function for detection time of a failure and its probable causes, an approximate loss function can be deduced for each failure-cause. Based on the value of the expected loss for each failure-cause, the risk priority metric (*RPM*) can be evaluated as the expected loss per unit time by multiplying the expected loss, which is determined by integration of loss function with its probability density function, and the occurrence rate of each failure-cause.

This manuscript has been organized as follows. Section 2 describes the proposed TD-FMEA model. In Section 3, a comparative analysis is conducted with the proposed TD-FMEA approach and traditional FMEA based on the design FMEA case of automotive leaf springs. Finally, we will draw conclusions and make suggestions for future research in Section 4.

2. Time-Dependent FMEA Model (TD-FMEA Model)

2.1. Modeling Procedure

The risk evaluation scheme of TD-FMEA proposed in this study is shown in Figure 2. First, probability density functions for occurrence time of failure $h_T(t)$, occurrence time of failure-cause $h_{T'}(t)$, and detection time $g_{S|T=t}(s)$ are defined. Next, the loss function $L(s, t)$ is defined. For evaluating the expected loss, it must be set parameter values $\lambda, \varepsilon, \mu, \alpha, \beta$, and θ . By integrating the loss function, we deduce the expected loss $E[L]$. Finally, by multiplying the occurrence rate of failure-cause ε by $E[L]$, we get the expected loss per unit time (RPM) for a focused failure-cause.

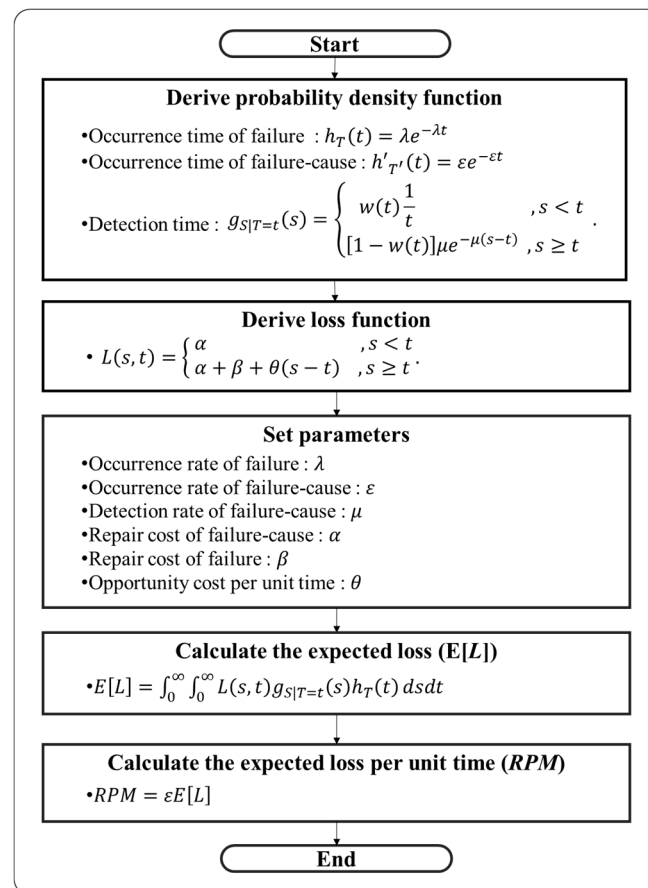


Figure 2. Risk evaluation scheme of time dependent FMEA (TD-FMEA).

2.2. Risk Evaluation Modeling

Consider a random variable T as an elapsed time from a failure-cause to the failure occurrence. Likewise, the detection time S is defined by the elapsed time between a failure-cause and its detection. By defining an appropriate loss function L as a function of the occurrence time T and detection time S , the expected loss $E[L]$ can be calculated accurately. A typical failure scenario is depicted in Figure 1.

2.2.1. Occurrence Time of a Failure and Its Failure-Cause

Under the assumption of a homogeneous Poisson process (HPP), the occurrence time T becomes a function of the failure occurrence rate λ . T can be considered exponentially distributed with mean $1/\lambda$, and its probability density function is expressed as

$$h_T(t) = \lambda e^{-\lambda t}, t > 0. \tag{1}$$

Additionally, T' is defined by the occurrence time of the failure-cause from its operation. As in Equation (1), T' can be considered as a function of the failure-cause occurrence rate ε with its average value $1/\varepsilon$. The corresponding probability density and cumulative distribution functions are

$$h'_{T'}(t) = \varepsilon e^{-\varepsilon t} \text{ and} \tag{2}$$

$$H'_{T'}(t) = 1 - e^{-\varepsilon t} \text{ with } t > 0. \tag{3}$$

2.2.2. Detection Time of a Failure-Cause

The probability density function of a corresponding failure-cause detection is generally assumed to be uniform before a failure occurrence, because a failure-cause is usually detected in accordance with the regularized detection schedule of a uniform time interval. Now, assume that we do not detect the failure-cause until the failure occurs. In the early stages of a failure, intensive detection will be attempted to detect failure-cause, so the probability density function of detection will be high at the initial state and will then gradually reduce. Thus, we considered an exponential function in this study, because it is the easiest to integrate and demonstrates excellent expansion. Therefore, probability density function of a failure-cause detection will be a case function conditioned by the time of occurrence.

Now, set up the following variables for obtaining the exact probability density function of detection time. Let us consider a failure and its failure-cause. Here, s is the elapsed time between occurrence and detection of the failure-cause. Similarly, t is the elapsed time between occurrence of failure and that of its failure-cause. As mentioned before, the conditional probability density function $g_{S|T=t}(s)$ is uniform in the domain where a detection time s is less than the given occurrence time t . Otherwise, $g_{S|T=t}(s)$ has an exponential form. Next, we have to determine the weight of the uniform and exponential section among the total probability 1. Let $w(t)$ be the cumulative probability of the uniform distribution; then, $1 - w(t)$ is the cumulative probability of the exponential distribution as shown in Figure 3. Thus, the conditional probability density function $g_{S|T=t}(s)$ is expressed as a function of the failure-cause detection rate μ , given the failure occurrence time $T = t$.

$$g_{S|T=t}(s) = \begin{cases} w(t) \frac{1}{t} & , s < t \\ [1 - w(t)] \mu e^{-\mu(s-t)} & , s \geq t \end{cases} \tag{4}$$

The function $g_{S|T=t}(s)$ may jump up at $s = t$. This is because more efforts are expected to be made to repair the failure and normalize the system at a time t . Thus, for $s = t$ with jump up coefficient c ,

$$c w(t) \frac{1}{t} = [1 - w(t)] \mu e^{-\mu(t-t)} = [1 - w(t)] \mu. \tag{5}$$

Rearrangement of Equation (5) yields

$$w(t) = \frac{\mu t}{c + \mu t}. \tag{6}$$

The weight function $w(t)$ equals zero when t is zero and becomes unity as t approaches infinity. This result is intuitively appropriate, since the probability of detection before failure would nearly

equal zero when t approaches zero, and as t becomes infinitely large, the detection probability must approach unity. Thus,

$$g_{S|T=t}(s) = \begin{cases} \frac{\mu}{c+\mu t} & , s < t \\ \frac{c\mu}{c+\mu t} e^{-\mu(s-t)} & , s \geq t \end{cases} \quad (7)$$

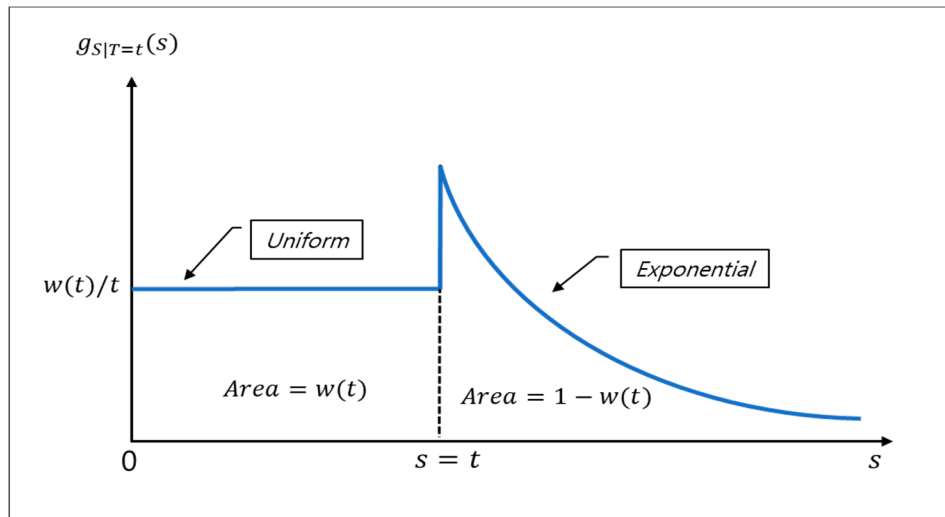


Figure 3. Conditional probability density function $g_{S|T=t}(s)$ of detection time s , given t of the failure occurrence time T .

2.2.3. Loss of Failure

If an inherent failure-cause exists within a system, there must be a cost associated with its elimination or prevention of the failure-cause. If a failure-cause is not detected until system failure occurs, it will add not only the failure-cause removal cost but also the system failure cost. The additional costs incurred as a result of system failure are the fixed cost and variable cost, i.e., a threshold cost and opportunity cost for system non-operation due to the system failure. The opportunity cost depends on the difference between failure-cause detection time s and failure occurrence time t . Let $L(s, t)$ be a loss function for a system with several failure-cause. As we mentioned above, the loss is only the failure-cause removal cost for $s < t$. However, for $s \geq t$, the loss is the sum of a failure-cause removal cost, threshold cost of the system failure, and an opportunity cost of the system non-operation proportional to $s - t$. That is,

$$L(s, t) = \begin{cases} \alpha & , s < t \\ \alpha + \beta + \theta(s - t) & , s \geq t \end{cases} \quad (8)$$

Here, α , β , and θ denotes a failure-cause removal cost, threshold cost of the system failure, and proportional factor of opportunity cost because of the system non-operation.

2.3. Loss Evaluation

2.3.1. Expected Value of Loss

The expected value of the loss function is calculated by integrating the loss function. From Equations (1), (4), and (8), the probability density function of failure occurrence time $h_T(t)$,

failure-cause detection time $g_{S|T=t}(s)$, and the loss function $L(s, t)$ are easily multiplied. Then, the expected value of the loss $E[L]$ is calculated by the following.

$$\begin{aligned}
 E[L] &= \int_0^\infty \int_0^\infty L(s, t) g_{S|T=t}(s) h_T(t) ds dt \\
 &= \int_0^\infty \int_0^t L(s, t) g_{S|T=t}(s) h_T(t) ds dt + \int_0^\infty \int_t^\infty L(s, t) g_{S|T=t}(s) h_T(t) ds dt \\
 &= \int_0^\infty \int_0^t \alpha \frac{\mu}{c + \mu t} \lambda e^{-\lambda t} ds dt + \int_0^\infty \int_t^\infty [\alpha + \beta + \theta(s - t)] \frac{c\mu}{c + \mu t} e^{-\mu(s-t)} \lambda e^{-\lambda t} ds dt \\
 &= \int_0^\infty \alpha \left[\int_0^t \frac{\mu}{c + \mu t} ds + \int_t^\infty \frac{c\mu}{c + \mu t} e^{-\mu(s-t)} ds \right] \lambda e^{-\lambda t} dt + \int_0^\infty \int_t^\infty [\beta + \theta(s - t)] \frac{c\mu}{c + \mu t} e^{-\mu(s-t)} \lambda e^{-\lambda t} ds dt \\
 &= \alpha + \left(\beta + \frac{\theta}{\mu} \right) \frac{c\lambda}{\mu} e^{\frac{c\lambda}{\mu}} E_1 \left(\frac{c\lambda}{\mu} \right)
 \end{aligned} \tag{9}$$

(See Appendix A)

For $x > 0$, $E_1(x)$ is the exponential integral function defined by

$$E_1(x) = \int_1^\infty \frac{e^{-xt}}{t} dt = \int_x^\infty \frac{e^{-t}}{t} dt = -\gamma - \ln x - \sum_{k=1}^\infty \frac{(-x)^k}{kk!}. \tag{10}$$

where $\gamma = \lim_{n \rightarrow \infty} \left(\sum_{k=1}^n \frac{1}{k} - \ln n \right) = 0.577 \dots$ is an irrational number called the Euler constant.

2.3.2. Risk-Prioritization Metric

Consider an occurrence of failure and failure-cause in a system. Suppose that a failure-cause of the failure occurs according to a homogeneous Poisson process (HPP) with a failure-cause occurrence rate ε . This statement is in fact equivalent to Equation (2). Finally, we propose the *RPM* compared with the *RPN* in the representative standard of FMEA. The *RPM* is easily calculated by

$$RPM = \varepsilon E[L] = \varepsilon \left[\alpha + \left(\beta + \frac{\theta}{\mu} \right) \frac{c\lambda}{\mu} e^{\frac{c\lambda}{\mu}} E_1 \left(\frac{c\lambda}{\mu} \right) \right]. \tag{11}$$

3. Application

3.1. Parameters Setting of RPM and RPN Values

FMEA of product design, performed by Santhosh and Vinodh [4] for an organization that manufactures automotive leaf springs, was adopted in this research as a case study to demonstrate the utility of the proposed TD-FMEA model. Table 1 describes the FMEA chart for design documented as part of this case study. The modified chart describes analysis of various failure causes—from FC₁₁ to FC₂₃—listed under column 1 with *O*, *S*, and *D*. Numerical values were assigned to parameters ε , λ , α , β , and θ , or simulations of the TD-FMEA model for design FMEA. A few of these parameter values were slightly modified as necessary to suit the proposed model. Values concerning the detection and occurrence rates— μ and ε —were obtained by modifying the corresponding ratings of factors *O* and *D*, respectively, in accordance with Table 2, which in turn, was modified with reference to the FMEA handbook [30].

Table 1. Parameter setting for simulations of the time dependent FMEA (TD-FMEA) model for design FMEA: As shown in Equation (11), there are many parameters such as failure-cause detection rate μ , failure-cause occurrence rate ε , failure occurrence rate λ , and coefficients α , β , and θ of loss function L . We set the parameters to compare risk prioritization metric (RPM) and risk prioritization number (RPN) by various simulations, fixing, and modifying each parameter.

Potential Failure-Causes (O, S, D)		Modified			Fixed			Variable			
		μ	ε	λ	Coefficients of Loss Function			λ	Coefficients of Loss Function		
					α	β	θ		α	β	θ
Insufficient specification of Thickness (5, 7, 6)	FC11	6.01-E-02	3.61-E-03	1.81-E-02	350	700	1000	1.81-E-02	400	800	1000
Insufficient room between plates (6, 7, 4)	FC12	2.72-E-01	1.81-E-02	1.81-E-02	350	700	1000	7.22-E-04	450	900	2000
Design aspect of Improper variation in length (4, 7, 5)	FC13	1.35-E-01	7.22-E-04	1.81-E-02	350	700	1000	1.93-E-01	100	200	2500
No. of layers not meeting Requirements (3, 6, 4)	FC21	2.72-E-01	9.60-E-05	1.81-E-02	350	600	1000	7.22-E-04	150	300	3000
Young's modulus of material changing with temperature (8, 6, 5)	FC22	1.35-E-01	1.93-E-01	1.81-E-02	350	600	1000	9.60-E-05	250	500	1500
Corner design of holding clamps (8, 6, 4)	FC23	2.72-E-01	1.93-E-01	1.81-E-02	350	600	1000	7.40-E-02	340	680	3500
Potential Failure mode		Reduced thickness of sheet									

μ : Failure-cause detection rate; ε : Failure-cause occurrence rate; λ : Failure mode occurrence rate.

Table 2. Standardization of parameters for failure-cause occurrence rate ε , failure occurrence rate λ , and failure-cause detection rate μ : The guideline is referenced by Ford Motor Company [30].

Guideline	Occurrence		Severity			Detection		
	Rank for RPN	ε, λ for RPM	Guideline	Rank for RPN	RPM	Guideline	Rank for RPN	μ for RPM
\geq in 2	10	1.00-E+00	Hazardous	10	$E[L]$	Absolute uncertainty	10	9.81-E-04
1 in 3	9	5.85-E-01	Serious	9		Very remote	9	3.10-E-03
1 in 8	8	1.93-E-01	Extreme	8		Remote	8	9.81-E-03
1 in 20	7	7.40-E-02	Major	7		Very low	7	2.69-E-02
1 in 80	6	1.81-E-02	Significant	6		Low	6	6.01-E-02
1 in 400	5	3.61-E-03	Moderate	5		Moderate	5	1.35-E-01
1 in 2000	4	7.22-E-04	Low	4		Moderately high	4	2.72-E-01
1 in 15,000	3	9.62-E-05	Minor	3		High	3	4.39-E-01
1 in 150,000	2	9.62-E-06	Very minor	2		Very high	2	7.65-E-01
\leq 1 in 1,500,000	1	9.62-E-07	None	1		Almost certain	1	1.00-E+00

Severity is not input of RPM, but the result of calculation such a name of expected value of loss $E[L]$.

In Table 2, occurrence rate of failure-cause and failure mode— ε and λ —for *RPM* are set to satisfy the given guideline such that cumulative probability of failure occurrence during unit time for the exponential distribution can be determined. Moreover, detection rate— μ for *RPM* is 1 over square-root of λ . This is because the effect of μ is opposite to that of λ , and μ is related to inspection policy compared to λ as an inherent property of the system. So, it assumes that the μ does not have dramatic range compared to λ . Parameters concerning the coefficient loss function— α , β and θ —were randomly assigned with reference to the *S* (severity) value of first column in Table 1. For parameters α , β , and θ , fixed and variable parameters were allocated to derive various simulation results.

3.2. Comparative Analysis of *RPM* and *RPN*

To illustrate the effectiveness of the proposed risk-evaluation technique, the above-described case study was used to analyze and compare results obtained using the proposed TD-FMEA model and conventional design FMEA techniques. The results are described in Table 3, that lists values of the conventional *RPN*, proposed *RPM*, and *E[L]* for each probable failure-cause in terms of both score and priority. To facilitate the robust evaluation of risks during the case study, results obtained for four cases ((a)–(d)) have been discussed herein considering, in each case, the effect of variation in the value of any one parameter among λ , α , β , and θ . Figure 4 shows the correlation of priority of *RPN* and *RPM* in Table 3, respectively, in four cases. The square root of R^2 is 0.8 or higher, it is determined that there is a strong correlation [31]. The square root of R^2 always satisfies $-1 \leq r \leq 1$, the positive correlation is $r > 0$, the negative correlation is $r < 0$. Moreover, when it is free, it becomes $r = 0$.

Table 3. Comparison between *RPN* of conventional FMEA model and *RPM* of TD-FMEA model for design FMEA: The priority of *RPN* and *RPM* is similar, so we may confirm the validity of the TD-FMEA model to some extent. (* set μ and ε to the modified values in Table 1).

Case	Failure-Causes	<i>RPN</i>		<i>RPM</i>		<i>E[L]</i>	
		Score	Priority	Score	Priority	Score	Priority
(a) Fixed λ, α, β and θ	FC11	210	2	22	3	6180	1
	FC12	168	4	17	4	958	4
	FC13	140	5	2	5	2103	2
	FC21	72	6	9·E−02	6	945	5
	FC22	240	1	401	1	2081	3
	FC23	192	3	182	2	945	5
(b) Fixed λ and Variable α, β and θ	FC11	210	2	23	4	6263	1
	FC12	168	4	29	3	1597	6
	FC13	140	5	3	5	4147	2
	FC21	72	6	2·E−01	6	1725	5
	FC22	240	1	532	1	2760	3
	FC23	192	3	428	2	2224	4
(c) Fixed α, β and θ , and Variable λ	FC11	210	2	22	3	6180	1
	FC12	168	4	7	4	404	4
	FC13	140	5	4	5	5465	2
	FC21	72	6	4·E−02	6	402	5
	FC22	240	1	74	2	383	6
	FC23	192	3	330	1	1713	3
(d) Variable λ, α, β and θ	FC11	210	2	23	3	6263	2
	FC12	168	4	10	4	551	4
	FC13	140	5	9	5	11,911	1
	FC21	72	6	3·E−02	6	289	6
	FC22	240	1	57	2	297	5
	FC23	192	3	897	1	4658	3

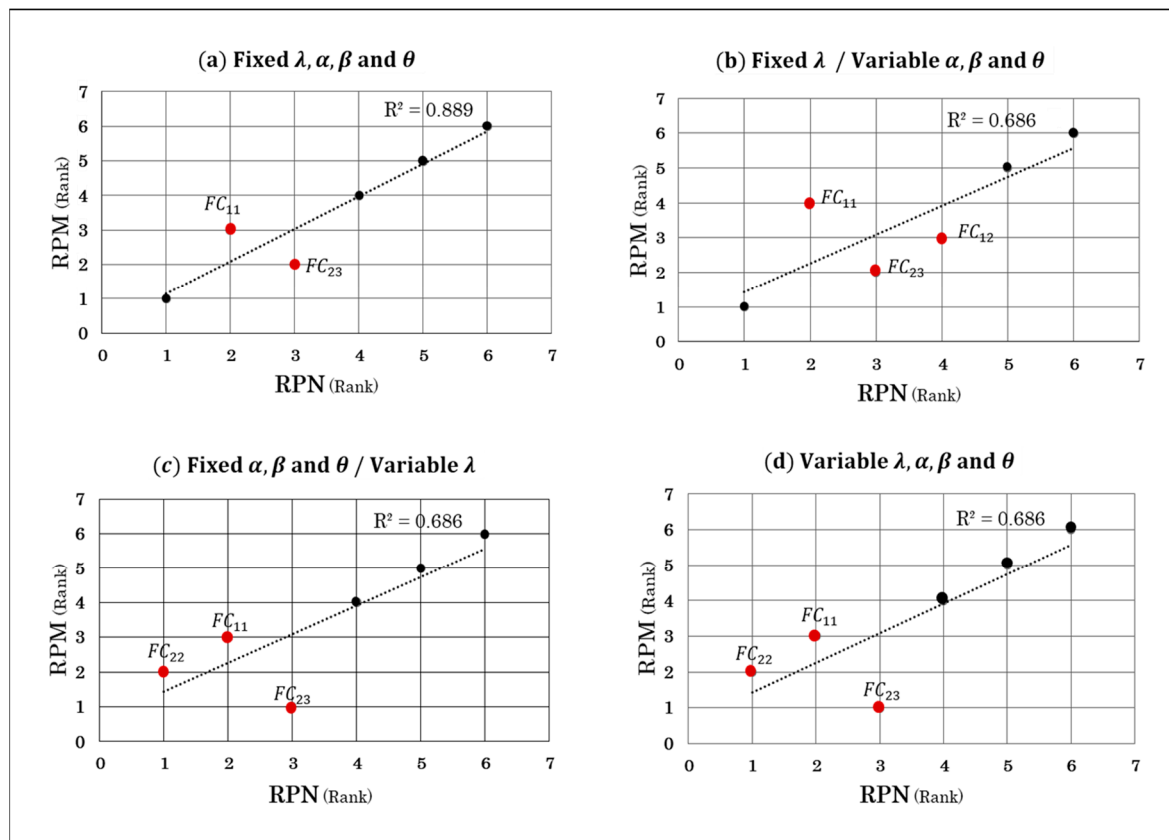


Figure 4. Rank correlation between *RPM* and *RPN* obtained by design FMEA: *RPM* and *RPN* are strongly correlated except for slight variations in priority rank. In this case, square root of R^2 is Spearman correlation coefficient, i.e., Pearson correlation coefficient of rank.

In Figure 4, regarding case (a), the square root of R^2 between *RPN* and *RPM* was 0.943, indicating a strong correlation. In Table 3, however, in terms of score, they are different. Based on *RPN* values, the FC_{22} (score = $8 \times 6 \times 5 = 240$) demonstrates the highest priority and can be considered the most critical risk closely followed by FC_{11} (score = 210) and FC_{23} (score = 192) ranked second and third, respectively. The difference in *RPN* scores corresponding to the FC_{22} and FC_{11} is 30 ($= 240 - 210$), whereas that between the FC_{11} and FC_{23} is 18 ($210 - 192$). This, however, does not imply that 30 equals two times 18 from the viewpoint of risk size. In the case of *RPM*, the FC_{22} (score = 401) demonstrates the highest priority and can be considered the most critical risk followed by FC_{23} (score = 182) and FC_{11} (score = 22) ranked second and third, respectively. The difference in score corresponding to the FC_{22} and FC_{23} is 219 ($401 - 182$), whereas that between the FC_{23} and FC_{11} is 160 ($182 - 22$). This means that 219 is about 1.37 times larger 160 from the viewpoint of risk size. Moreover, as depicted in Figure 4 for case (a), the FC_{11} and FC_{23} are prioritized as three and two, respectively, when employing the *RPM*-based approach, whereas the same failure-causes are prioritized as two and three, respectively, in accordance with *RPN* values. This is because the occurrence rate ϵ for the FC_{23} is considerably higher compared to that for FC_{11} , although the parameter μ is not significantly different for both risks (refer Table 1). This result is also reflected in *RPM* scores corresponding to the two cases. The score corresponding to the FC_{23} (score = 182) equals eight times that corresponding to FC_{11} (score = 22); that is, the loss incurred per hour in the event of a failure-caused by FC_{23} would be eight times that incurred in the event of a failure that was caused by FC_{11} . On the other hand, this result is different in terms of $E[L]$. As described in Table 3, the FC_{23} with $E[L] = 945$ assumes the least priority. This implies that there is a high probability of detecting the FC_{23} before the failure occurs; thus, its corresponding $E[L]$ score is low.

Regarding case (b), in Table 3, FC_{22} , FC_{13} , and FC_{21} are consistently assigned priorities of 1, 5, and 6, respectively, using both the *RPN*- and *RPM*-based approaches. As depicted in Figure 4 for case (b), the square root of R^2 between *RPN* and *RPM* was 0.829, indicating a strong correlation. Additionally, the FC_{11} , FC_{23} , and FC_{12} are assigned of 4 (score = 23), 2 (score = 428), and 3 (score = 29), respectively, when employing the *RPM*-based approach, whereas the same failure-causes are prioritized as two (score = 210), 3 (score = 192), and 4 (score = 168), respectively, when employing the *RPN*-based approach. This is because, as described in Table 1, variable parameters α , β , and θ for FC_{23} and FC_{12} exceed those for fixed parameters. On the other hand, in terms of $E[L]$, the FC_{11} with the smallest value of parameter μ assumes the highest priority, whereas risk FC_{12} with the largest values of μ assumes the lowest priority (refer Table 1).

In case (c), compared to *RPM*-based results obtained for case (a) (refer Figure 4), it can be realized that the *RPM*-based priority assigned to the FC_{22} changes from one to two while that of the FC_{23} changes from two to one. This is because the value of parameter λ for the FC_{23} exceeds that for the FC_{22} by a fairly large magnitude (refer Table 1). In contrast, in terms of $E[L]$, the FC_{11} with medium value of λ and the smallest value of μ assumes the highest priority, whereas the FC_{22} with small value of λ and large value of μ is assigned the lowest priority.

Lastly, in case (d), compared to *RPM*-based results, for case (d) are identical to those obtained for case (c) in terms of priority, and they are quite similar on the score side. In Figure 4, the square root of R^2 between *RPN* and *RPM* was also 0.829, indicating a strong correlation. On the other hand, in terms of $E[L]$, results are quite different. For example, for the FC_{13} , the score of $E[L]$ is more than double in case (d) than in case (c). This is because the λ and θ increased at the same time for case (d) (refer Table 3).

In most cases, the rankings cannot be fully matched because the method of derivation of *RPN* and *RPM* is completely different. Since *RPN* is not a perfect risk measurement tool currently, it is difficult to distinguish the superiority of *RPN* and *RPM* for the difference in rank. However, since correlation coefficients are high enough (higher than 0.8 for most cases), it is hard to say that *RPN* and *RPM* make a significant difference. *RPM* means the size of risk or loss unlike *RPN*, so *RPM* may have a wider range of applications than *RPN*. Above all, the parameters O , S , and D of *RPN* have over-dependence on expert intuition and experience instead of scientific methods for evaluation. However, the parameters of *RPM* are derived from statistical inference (ε , λ , and μ) and cost analysis (α , β , and θ). Thus, we may say the *RPM* measured by TD-FMEA model is more objective than *RPN* evaluated by the conventional FMEA model.

4. Conclusions

So far, we have proposed a time-dependent FMEA model (TD-FMEA model) and obtained an expected loss value $E[L]$ according to the occurrence of failure-cause through accurate calculation (Equation (9)). Then, we derived risk prioritization metric (*RPM*), which is a defined index measuring the risk of failure-cause in this study, multiplying by the failure-cause occurrence rate ε and the expected loss value $E[L]$ (Equation (11)).

The mathematical model proposed in this study performs an associated calculation on system failure, failure-cause, and its detection. The probability density function of failure and failure-cause are exponential by homogeneous Poisson process (HPP) assumption (Equations (1) and (2)), and that of failure-cause detection is a case function combined in a uniform and exponential manner (Equation (4)). The loss function is also a case function conditioned by detection time of failure-cause and occurrence time of failure (Equation (8)). Time-dependent probabilistic approach pursues logical improvement compared to previous models. Conventional *RPN* approach assumes that O (occurrence of failure), S (severity of failure), and D (detection of failure-cause) are independent. However, *RPM* in our model does not assume the independence because it combines failure occurrence rate, detection rate of failure-cause, and loss function to derive the risk of failure-cause. Table 4 compared the traditional FMEA and our TD-FMEA model.

Table 4. Comparison of traditional FMEA and TD-FMEA.

Division	Conventional FMEA	TD-FMEA
	<i>O, S, and D</i>	$\epsilon, \lambda, \mu, \alpha, \beta, \text{ and } \theta$
Risk Parameter (i)	<ul style="list-style-type: none"> Expert intuition and experience Relative order-based Range from 1 to 10 for <i>O, S, and D</i> 	<ul style="list-style-type: none"> Statistical inference ($\epsilon, \lambda, \text{ and } \mu$) and cost analysis ($\alpha, \beta \text{ and } \theta$) No limit of range
	RPN score (ranking of $O \times S \times D$)	RPM score ($\epsilon E[L]$)
Risk Measure (ii)	<ul style="list-style-type: none"> Qualitative Subjective Relative Risk Priority 	<ul style="list-style-type: none"> Quantitative Objective Exact Loss per Unit Time

O: Occurrence; S: Severity; D: Detection;
 ϵ : Occurrence rate of failure-cause; λ : Occurrence rate of failure;
 μ : Detection rate of failure-cause; α : Repair cost of failure-cause (coefficient of loss function);
 β : Repair cost of failure (coefficient of loss function);
 θ : Opportunity cost per unit time because of the system down (coefficient of loss function).

The *RPM* derived in this way provides room to supplement the disadvantages of traditional risk prioritization number (*RPN*). The coefficient of determination R^2 between the priority of *RPM* and *RPN* has a range of 0.686~0.889 in our example (Figure 4). That is the rank correlation has a range of 0.828~0.943, so that *RPM* and *RPN* have very strong correlations. From this, we can say that the validity of our model has been empirically proven. Furthermore, our model has the advantage that the *RPM* value represents the relative size of the actual risk. In contrast, the product of *O, S, and D* derived from *RPN* of conventional approaches is only an auxiliary value to derive the priority without having any substantial meaning (Table 3). Utility of both indicators $E[L]$ and *RPM* with regard to evaluation of the risk associated with each failure has been described in great detail in Section 3 of this paper. For a reasonable calculation, we provide a standardization of parameters for failure-cause occurrence rate ϵ , failure occurrence rate λ , and failure-cause detection rate μ , which is a variation of our model from the guideline of Ford Motor Company (Table 2). In addition, the results of the sensitivity analysis of *RPM* can be found in Appendix B.

In future endeavors, our future prospect is to examine actual cases based on actual parameters. The purpose of the study is to derive correlation coefficients of *RPN* and *RPM* rankings to infer the validity of *RPM*, and to verify the effectiveness by deriving risks from *RPM* values. Moreover, we intend to focus on development of an FMEA risk-assessment methodology for a single failure with multiple causes along with determination of an optimal inspection period to enhance the detection rate based on $E[L]$ values. In addition, if the failure-causes are analyzed hierarchically, a time-dependent probabilistic model will be developed based on undetected time.

- (i) In traditional FMEAs, risks can be assessed on a ranking basis, making it an easy-to-use approach when data is difficult to obtain. In the big data world, however, the application of a numerical-based TD-FMEA approach will enable more accurate assessment of risk.
- (ii) In traditional FMEAs, the results of a risk assessment may depend on the subjective opinion of the expert. On the other hand, in the case of the TD-FMEA approach, the objectivity of the result is secured based on probability.

Author Contributions: Conceptualization, H.-a.J. and S.M.; Methodology, H.-a.J. and S.M.; Modeling, S.M.; Validation H.-a.J. and S.M.; Writing—original draft preparation, H.-a.J. and S.M.; Writing—Review and Editing, H.-a.J.; and S.M.; Funding Acquisition, H.-a.J. and S.M.

Funding: This work was supported by the National Research Foundation of Korea (NRF) in a grant funded by the Korean government (MSIT) (No. 2019R1G1A1010335 and 2017R1C1B5017491).

Conflicts of Interest: The authors declare no conflict of interest.

Appendix A

$$\begin{aligned}
 E[L] &= \int_0^\infty \int_0^\infty L(s, t) g_{S|T=t}(s) h_T(t) ds dt \\
 &= \int_0^\infty \int_0^t L(s, t) g_{S|T=t}(s) h_T(t) ds dt + \int_0^\infty \int_t^\infty L(s, t) g_{S|T=t}(s) h_T(t) ds dt \\
 &= \int_0^\infty \int_0^t \alpha \frac{\mu}{c + \mu t} \lambda e^{-\lambda t} ds dt + \int_0^\infty \int_t^\infty [\alpha + \beta + \theta(s - t)] \frac{c\mu}{c + \mu t} e^{-\mu(s-t)} \lambda e^{-\lambda t} ds dt \\
 &= \int_0^\infty \alpha \left[\int_0^t \frac{\mu}{c + \mu t} ds + \int_t^\infty \frac{c\mu}{c + \mu t} e^{-\mu(s-t)} ds \right] \lambda e^{-\lambda t} dt + \int_0^\infty \int_t^\infty [\beta + \theta(s - t)] \frac{c\mu}{c + \mu t} e^{-\mu(s-t)} \lambda e^{-\lambda t} ds dt.
 \end{aligned}
 \tag{A1}$$

$$\begin{aligned}
 & \tag{I} \\
 & \int_0^\infty \alpha \left[\int_0^t \frac{\mu}{c + \mu t} ds + \int_t^\infty \frac{c\mu}{c + \mu t} e^{-\mu(s-t)} ds \right] \lambda e^{-\lambda t} dt \\
 &= \int_0^\infty \alpha \left[\int_0^t \frac{\mu}{c + \mu t} ds + \int_0^\infty \frac{c\mu}{c + \mu t} e^{-\mu \tilde{s}} d\tilde{s} \right] \lambda e^{-\lambda t} dt; \tilde{s} = s - t \\
 &= \int_0^\infty \alpha \left(\frac{\mu t}{c + \mu t} + \frac{c}{c + \mu t} \right) \lambda e^{-\lambda t} dt \\
 &= \alpha \frac{c + \mu t}{c + \mu t} \\
 &= \alpha.
 \end{aligned}
 \tag{A2}$$

$$\begin{aligned}
 & \tag{II} \\
 & \int_0^\infty \int_t^\infty [\beta + \theta(s - t)] \frac{c\mu}{c + \mu t} e^{-\mu(s-t)} \lambda e^{-\lambda t} ds dt \\
 &= \int_0^\infty \frac{c}{c + \mu t} \lambda e^{-\lambda t} dt \int_t^\infty [\beta + \theta(s - t)] \mu e^{-\mu(s-t)} ds \\
 &= \int_0^\infty \frac{c\lambda}{c + \mu t} e^{-\lambda t} dt \int_0^\infty [\beta + \theta \tilde{s}] \mu e^{-\mu \tilde{s}} d\tilde{s}; \tilde{s} = s - t \\
 &= \int_0^\infty \frac{c\lambda}{c + \mu t} e^{-\lambda t} dt \left[(\beta + \theta \tilde{s}) (-e^{-\mu \tilde{s}}) \Big|_0^\infty - \theta \left(\frac{1}{\mu} e^{-\mu \tilde{s}} \right) \Big|_0^\infty \right]; \text{integration by parts} \\
 &= \left(\beta + \frac{\theta}{\mu} \right) \int_0^\infty \frac{c\lambda}{c + \mu t} e^{-\lambda t} dt \\
 &= \left(\beta + \frac{\theta}{\mu} \right) \int_{\frac{c\lambda}{\mu}}^\infty \frac{\mu}{\tau} e^{\frac{c\lambda}{\mu} - \tau} \frac{1}{\lambda} d\tau; \tau = \frac{c\lambda}{\mu} + \lambda t = \frac{\lambda}{\mu} (c + \mu t) \\
 &= \left(\beta + \frac{\theta}{\mu} \right) \frac{c\lambda}{\mu} e^{\frac{c\lambda}{\mu}} \int_{\frac{c\lambda}{\mu}}^\infty \frac{e^{-\tau}}{\tau} d\tau \\
 &= \left(\beta + \frac{\theta}{\mu} \right) \frac{c\lambda}{\mu} e^{\frac{c\lambda}{\mu}} E_1 \left(\frac{c\lambda}{\mu} \right).
 \end{aligned}
 \tag{A3}$$

For $x > 0$, $E_1(x)$ is the exponential integral function defined by

$$E_1(x) = \int_1^\infty \frac{e^{-xt}}{t} dt = \int_x^\infty \frac{e^{-t}}{t} dt = -\gamma - \ln x - \sum_{k=1}^\infty \frac{(-x)^k}{kk!},
 \tag{A4}$$

where $\gamma = \lim_{n \rightarrow \infty} \left(\sum_{k=1}^n \frac{1}{k} - \ln n \right) = 0.577 \dots$ is an irrational number called the Euler constant. Therefore,

$$E[L] = \alpha + \left(\beta + \frac{\theta}{\mu} \right) \frac{c\lambda}{\mu} e^{\frac{c\lambda}{\mu}} E_1 \left(\frac{c\lambda}{\mu} \right).
 \tag{A5}$$

Appendix B

A sensitivity analysis was performed in this study to investigate the influence of distribution-parameter values on those of *RPM*. Sensitivity of *RPM* values to values of parameters— μ and λ —can be readily analyzed. In this study, sensitivity of the value of *RPM* was analyzed by assigning parameters ε , α , β , and θ with constant of 1.81E−02, 200, 1000, and 1200, respectively. Variations in

the value of *RPM* corresponding to changes in values of μ and λ are listed in Table A1 and depicted in Figure A1, respectively. Results obtained demonstrate that smaller values of μ result in enhanced sensitivity of *RPM*. Figure A1a demonstrates that the value of *RPM* steeply increases with reduction in the value of μ . Secondly, as depicted in Figure A1b, it can be realized that the value of *RPM* is nearly insensitive to small values of λ , and that the corresponding sensitivity increases with increase in the value of λ .

Figure A1 demonstrates that the maximum value of *RPM* is realized for the case wherein $\mu = 10$ and $\lambda = 10$. This implies that maximization of a given risk of failure with the corresponding failure-cause is hardly detectable whilst having a high occurrence probability. As depicted in Figure A1, there exists a big difference between *RPM* values obtained for each μ . This can be verified in terms of the graph slope. In Figure A1a, the difference between *RPM* values is large for cases with $\mu = 10$ and λ assuming values in the range of 2–7. On the other hand, the difference between *RPM* values is small when $\mu = 1$ and λ assumes values in the range of 1–6. This implies that the *RPM* value does not demonstrate much difference when the failure probability is either very high or very low. Inferences drawn from the above sensitivity analysis are that (i) each failure-cause with a high occurrence probability must be taken care of; and (ii) a cause with a small occurrence probability need not be assigned high priority.

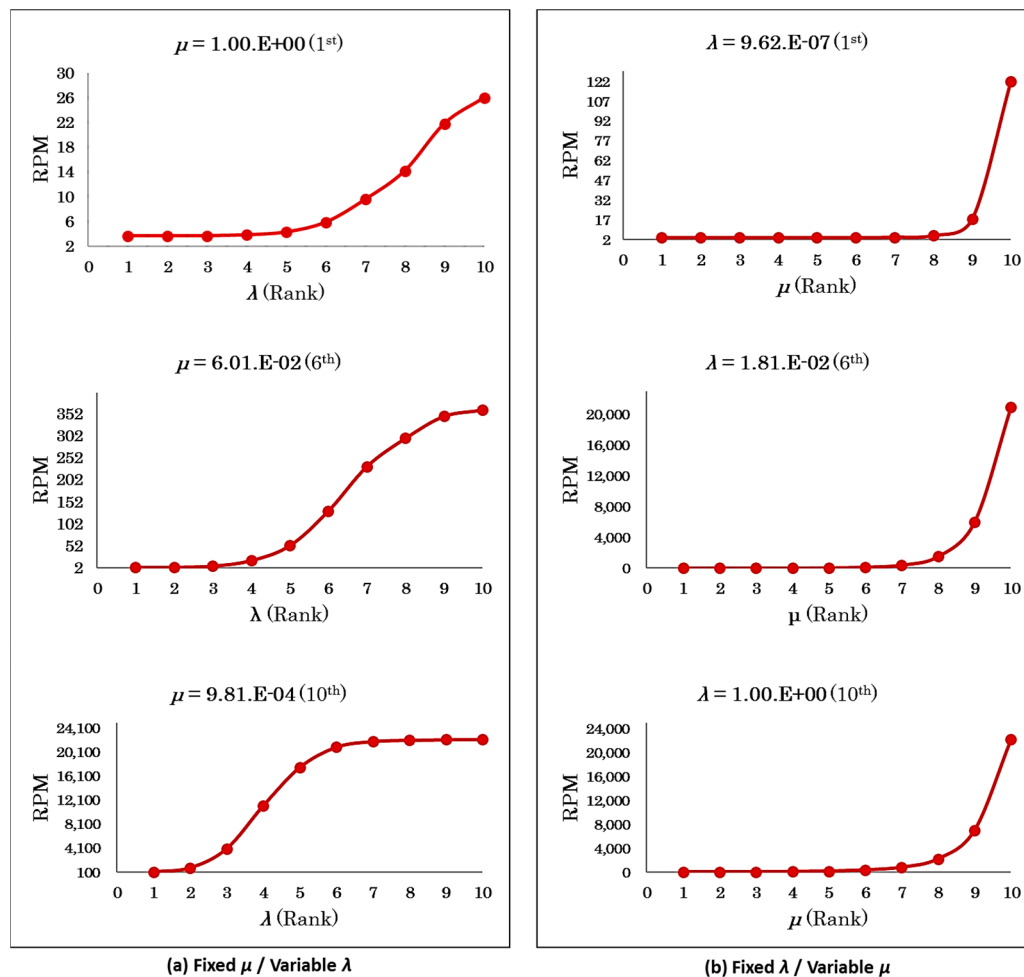


Figure A1. Risk-prioritization metric (*RPM*) graph with respect to the failure occurrence rate λ and failure-cause detection rate μ ($c = 1$, $\varepsilon = 0.0181$, $\alpha = 200$, $\beta = 1000$, and $\theta = 1200$). (a) *RPM* as a function of λ draws S-curve, and (b) *RPM* of μ increases rapidly more than exponential. Thus, the *RPM* is more sensitive to μ than λ .

Table A1. Risk-prioritization metric (RPM) table with respect to the failure occurrence rate λ and failure-cause detection rate μ ($c = 1, \varepsilon = 0.0181, \alpha = 200, \beta = 1000,$ and $\theta = 1200$).

	μ	1st	2nd	3rd	4th	5th	6 th	7th	8th	9th	10th
λ		1.00·E+00	7.65·E-01	4.39·E-01	2.72·E-01	1.35·E-01	6.01·E-02	2.69·E-02	9.81·E-03	3.10·E-03	9.81·E-04
1st	9.62·E-07	3.6	3.6	3.6	3.6	3.6	3.7	3.9	5.2	17.6	122.3
2nd	9.62·E-06	3.6	3.6	3.6	3.7	3.7	4.1	5.5	15.6	101.8	779.1
3rd	9.62·E-05	3.7	3.7	3.7	3.8	4.4	6.7	16.6	81.7	582.8	3957.5
4th	7.22·E-04	3.8	3.9	4.2	4.8	7.5	19.1	65.1	335.4	2070.7	11,132.7
5th	3.61·E-03	4.3	4.5	5.7	8.0	17.0	53.0	182.3	833.3	4159.8	17,546.2
6th	1.81·E-02	5.9	6.8	10.5	17.3	42.4	131.6	405.0	1519.6	5981.7	20,942.4
7th	7.40·E-02	9.6	11.9	20.3	34.9	83.5	232.4	621.3	1965.1	6720.4	21,883.9
8th	1.93·E-01	14.2	17.9	30.9	52.1	116.8	296.2	725.7	2119.6	6912.5	22,092.6
9th	5.85·E-01	21.9	27.3	45.4	72.7	149.7	345.8	791.1	2198.9	6999.4	22,182.3
10th	1.00·E+00	26.0	32.2	52.0	81.1	160.9	360.0	807.3	2216.5	7017.6	22,204.6

References

1. Stamatis, D.H. *Failure Mode and Effect Analysis: FMEA from Theory to Execution*, 2nd ed.; ASQ Quality Press: Milwaukee, WI, USA, 1995.
2. Liu, H.; Liu, L.; Liu, N. Risk evaluation approaches in failure mode and effects analysis: A literature review. *Expert Syst. Appl.* **2013**, *40*, 828–838. [[CrossRef](#)]
3. Geum, Y.; Cho, Y.; Park, Y. A systematic approach for diagnosing service failure: Service-specific FMEA and grey relational analysis approach. *Math. Comput. Model.* **2011**, *54*, 3126–3142. [[CrossRef](#)]
4. Santhosh, D.; Vinodh, S. Application of FMEA to an automotive leaf spring manufacturing organization. *TQM J.* **2012**, *24*, 260–274.
5. Yazdi, M.; Daneshvar, S.; Setareh, H. An extension to Fuzzy Developed Failure Mode and Effects Analysis (FDFMEA) application for aircraft landing system. *Saf. Sci.* **2017**, *98*, 113–123. [[CrossRef](#)]
6. Wang, W.; Liu, X.; Qin, Y.; Fu, Y. A risk evaluation and prioritization method for FMEA with prospect theory and Choquet integral. *Saf. Sci.* **2018**, *110*, 152–163. [[CrossRef](#)]
7. Fattahi, R.; Khalilzadeh, M. Risk evaluation using a novel hybrid method based on FMEA, extended MULTIMOORA, and AHP methods under fuzzy environment. *Saf. Sci.* **2018**, *102*, 290–300. [[CrossRef](#)]
8. Mentés, A.; Ozen, E. A hybrid risk analysis method for a yacht fuel system safety. *Saf. Sci.* **2015**, *79*, 94–104. [[CrossRef](#)]
9. Zhou, Q.; Thai, V.V. Fuzzy and grey theories in failure mode and effect analysis for tanker equipment failure prediction. *Saf. Sci.* **2016**, *83*, 74–79. [[CrossRef](#)]
10. Maniram Kumar, A.; Rajakarunakaran, S.; Pitchipoo, P.; Vimalasan, R. Fuzzy based risk prioritisation in an auto LPG dispensing station. *Saf. Sci.* **2018**, *101*, 231–247. [[CrossRef](#)]
11. Rhee, S.J.; Ishii, K. Using cost based FMEA to enhance reliability and serviceability. *Adv. Eng. Inform.* **2003**, *17*, 179–188. [[CrossRef](#)]
12. Dong, C. Failure mode and effects analysis based on fuzzy utility cost estimation. *Int. J. Qual. Reliab. Manag.* **2007**, *24*, 958–971. [[CrossRef](#)]
13. Von Ahsen, A. Cost-oriented failure mode and effects analysis. *Int. J. Qual. Reliab. Manag.* **2008**, *25*, 466–476. [[CrossRef](#)]
14. Parracho Sant'Anna, A. Probabilistic priority numbers for failure modes and effects analysis. *Int. J. Qual. Reliab. Manag.* **2012**, *29*, 349–362. [[CrossRef](#)]
15. Certa, A.; Hopps, F.; Inghilleri, R.; La Fata, C.M. A Dempster-Shafer Theory-based approach to the Failure Mode, Effects and Criticality Analysis (FMECA) under epistemic uncertainty: Application to the propulsion system of a fishing vessel. *Reliab. Eng. Syst. Saf.* **2017**, *159*, 69–79. [[CrossRef](#)]
16. Huang, J.; Li, Z.; Liu, H. New approach for failure mode and effect analysis using linguistic distribution assessments and TODIM method. *Reliab. Eng. Syst. Saf.* **2017**, *167*, 302–309. [[CrossRef](#)]
17. Catelani, M.; Ciani, L.; Venzi, M. Failure modes, mechanisms and effect analysis on temperature redundant sensor stage. *Reliab. Eng. Syst. Saf.* **2018**, *180*, 425–433. [[CrossRef](#)]
18. Kim, K.O.; Zuo, M.J. General model for the risk priority number in failure mode and effects analysis. *Reliab. Eng. Syst. Saf.* **2018**, *169*, 321–329. [[CrossRef](#)]
19. Ding, X.; Su, Q.; You, J.; Liu, H. Improving risk evaluation in FMEA with a hybrid multiple criteria decision making method. *Int. J. Qual. Reliab. Manag.* **2015**, *32*, 763–782.
20. Mohsen, O.; Fereshteh, N. An extended VIKOR method based on entropy measure for the failure modes risk assessment—A case study of the geothermal power plant (GPP). *Saf. Sci.* **2017**, *92*, 160–172. [[CrossRef](#)]
21. Lo, H.; Liou, J.J.H.; Huang, C.; Chuang, Y. A novel failure mode and effect analysis model for machine tool risk analysis. *Reliab. Eng. Syst. Saf.* **2019**, *183*, 173–183. [[CrossRef](#)]
22. Yousefi, S.; Alizadeh, A.; Hayati, J.; Baghery, M. HSE risk prioritization using robust DEA-FMEA approach with undesirable outputs: A study of automotive parts industry in Iran. *Saf. Sci.* **2018**, *102*, 144–158. [[CrossRef](#)]
23. Sharma, R.K.; Sharma, P. System failure behavior and maintenance decision making using, RCA, FMEA and FM. *J. Qual. Maint. Eng.* **2010**, *16*, 64–88. [[CrossRef](#)]
24. Guimarães, A.C.F.; Lapa, C.M.F.; Moreira, M.D.L. Fuzzy methodology applied to Probabilistic Safety Assessment for digital system in nuclear power plants. *Nucl. Eng. Des.* **2011**, *241*, 3967–3976. [[CrossRef](#)]

25. Pillay, A.; Wang, J. Modified failure mode and effects analysis using approximate reasoning. *Reliab. Eng. Syst. Saf.* **2003**, *79*, 69–85. [[CrossRef](#)]
26. Carmignani, G. An integrated structural framework to cost-based FMECA: The priority-cost FMECA. *Reliab. Eng. Syst. Saf.* **2009**, *94*, 861–871. [[CrossRef](#)]
27. Zammori, F.; Gabrielli, R. ANP/RPN: A Multi Criteria Evaluation of the Risk Priority Number. *Qual. Reliab. Engng. Int.* **2012**, *28*, 85–104. [[CrossRef](#)]
28. Peeters, J.F.W.; Basten, R.J.I.; Tinga, T. Improving failure analysis efficiency by combining FTA and FMEA in a recursive manner. *Reliab. Eng. Syst. Saf.* **2018**, *172*, 36–44. [[CrossRef](#)]
29. Jang, H.A.; Lee, M.K.; Hong, S.H.; Kwon, H.M. Risk Evaluation Based on the Hierarchical Time Delay Model in FMEA. *J. Korean Soc. Qual. Manag.* **2016**, *44*, 373–388. [[CrossRef](#)]
30. Ford Design Institute. *FMEA Hand Book Version 4.1*; Ford Design Institute: Dearborn, MI, USA, 2004; p. 290.
31. Evans, J.D. *Straightforward Statistics for the Behavioral Sciences*; Thomson Brooks/Cole Publishing Co.: Belmont, CA, USA, 1996.



© 2019 by the authors. Licensee MDPI, Basel, Switzerland. This article is an open access article distributed under the terms and conditions of the Creative Commons Attribution (CC BY) license (<http://creativecommons.org/licenses/by/4.0/>).